Research paper

Preparation and characterization of sterile sub-200 nm meso-tetra(4-hydroxylphenyl)porphyrin-loaded nanoparticles for photodynamic therapy

Yvette Niamien Konan[a], Radovan Cerny[b], Joselyne Favet[c], Myriam Berton[a,1], Robert Gurny[a,*], Eric Allémann[a,2]

[a]School of Pharmacy, University of Geneva, Geneva, Switzerland
[b]Laboratory of Crystallography, University of Geneva, Geneva, Switzerland
[c]Laboratory of Microbacteriology, University of Geneva, Geneva, Switzerland

Abstract

A photosensitizer, meso-tetra(4-hydroxyphenyl)porphyrin, was incorporated into sub-150 nm nanoparticles using the emulsification-diffusion technique in order to perform sterilization by filtration using 0.22 μm membranes. The three selected polyesters (poly(D,L-lactide-co-glycolide), (50:50 PLGA, 75:25 PLGA) and poly(D,L-lactide (PLA)) for the nanoparticle production were all amorphous in nature and have similar molecular weights but different copolymer molar ratios. The influence of the copolymer molar ratio and the theoretical drug loading was investigated in terms of particle size, drug loading, entrapment efficiency and surface characteristics. With all the polymers used, sub-150 nm nanoparticles were produced with good reproducibility and narrow size distributions irrespective of both the polymer nature and the theoretical drug loading. After purification by cross-flow filtration, the nanoparticle suspensions were sterilized by membrane filtration and freeze-dried in the presence of a lyoprotectant (trehalose). For all types of nanoparticles, complete redispersion in various media could be obtained. All final freeze-dried products were refiltrable on a 0.22 μm membrane and were stable in terms of mean particle size and drug loading over a period up to 6 months. The effective drug loading increased at higher theoretical drug loading, the entrapment efficiency was however decreased. The same trend was observed with the three polyesters. The sterility of the final freeze-dried nanoparticles was confirmed by the results of the sterility testing which showed no bacterial contamination.
© 2002 Elsevier Science B.V. All rights reserved.

Keywords: Nanoparticles; Poly(D,L-lactide); Poly(D,L-lactide-co-glycolide); Sterile filtration; Photosensitizer; Meso-tetra(p-hydroxyphenyl)porphyrin; P-THPP

1. Introduction

Photodynamic therapy (PDT) is based on the accumulation of a photosensitizer (PS) in malignant tissues followed by illumination with light at an appropriate wavelength inducing photochemical reactions that result in tissue destruction. In several studies involving porphyrin-based PS, it has been shown that a correlation exists between PS tumor uptake and hydrophobicity. Indeed, it has been found that the retention of these PS in tumor cells increased with decreasing polarity [1,2]. However, high partition coefficient values (increased hydrophobicity) are related to PS insolubility, with the drawback of impeding the use of physiologically acceptable aqueous vehicles for intravenous administration. In recent years, the development of delivery systems allowing the intravenous administration of hydrophobic PS has received increasing attention. Several research strategies such as chemical conjugation with various water-soluble polymers [3,4] and encapsulation into colloidal carriers have been considered for the parenteral administration of hydrophobic PS with the additional aim of enhancing their selectivity. These colloidal carriers include liposomes [5,6], emulsions [7,8], polymeric micelles [9] and nanoparticles [10–14]. The rationale for using such delivery systems is related to their targeting ability [15,16]. In many cases, tumor tissues are supplied by a leaky neovasculature with an incomplete endothelial barrier and have a poor lymphatic drainage. This

* Corresponding author. School of Pharmacy, University of Geneva, 30, Quai Ernest-Ansermet, CH-1211 Geneva 4, Switzerland. Tel.: +41-22-702-6146; fax: +41-22-702-6567.
 E-mail address: robert.gurny@pharm.unige.ch (R. Gurny).
[1] Present address: Novartis S.A., Bas, Switzerland.
[2] Present address: Bracco Research S.A., CH-1228 Plan-les-Ouates, Geneva, Switzerland.
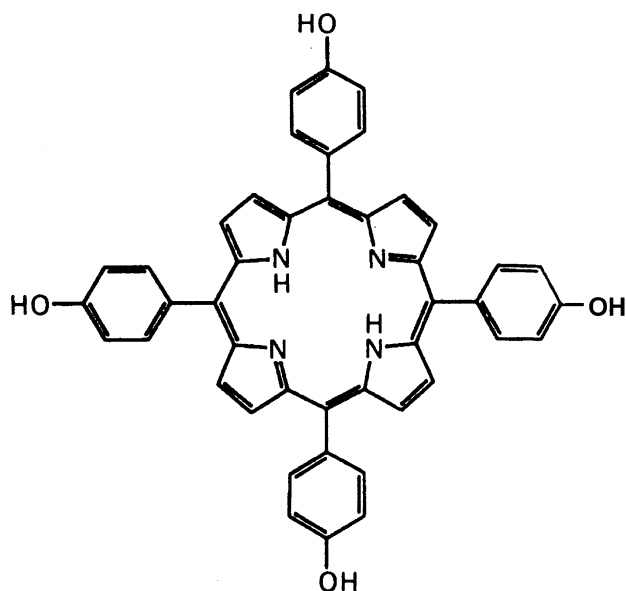
Fig. 1. Chemical structure of p-THPP (molecular weight: 678.76).

phenomenon is known as an 'enhanced permeability and retention effect' [17,18]. These tumor characteristics provide an opportunity for the colloidal carriers to reach their target site by diffusion (passive targeting) [19]. It has been demonstrated that passive targeting is limited to carriers with a size of around 100 nm [18,20]. With regard to nanoparticles, such particle sizes can be obtained by adapting manufacturing processes such as the salting-out method [21], the emulsification-diffusion technique [22] and the nanoprecipitation method [23]. In addition, as reported in a previous study [21], sub-200 nm nanoparticles present the advantage of being sterilized by membrane filtration. Surprisingly, although the small size of these drug carriers is likely to maximize their targeting ability in PDT, few studies have addressed the issue of the small particle size effect.

The aim of the present study was to prepare sterile sub-200 nm nanoparticles loaded with meso-tetra(p-hydroxy-phenyl)porphin, one among several second-generation photosensitizers of known composition, which can be potentially used in PDT of cancer as an alternative to Photofrin® II, a first-generation PS commonly used in PDT [24,25]. These nanoparticles, which were produced by the emulsification-diffusion technique, were subsequently intended for in vitro PDT study on EMT-6 mouse mammary tumor cells. As clinical applicability of these particles was considered of primary importance, poly(D,L-hydroxy acid) polymers were selected in view of their biodegradability and biocompatibility [26]. In addition, the possibility of modulating the drug release and the degradation rate of the particles is offered by choosing the appropriate polymer [27]. Hence, in the present study, in order to assess the influence of the monomer ratio on the properties of the nanoparticles, the selected polyesters (50:50 PLGA, 75:25 PLGA, PLA) had similar molecular weights (13 000–19 000 Da) and

crystallinities but exhibited different copolymer molar ratios. The particles were compared with respect to size, surface characteristics, drug loading and entrapment efficiency. The influence of the theoretical drug loading on the nanoparticle characteristics was also investigated.

2. Materials and methods

2.1. Materials

Poly(D,L-lactide-co-glycolide) (PLGA) with copolymer ratios of 50:50 PLGA (Resomer® RG502, molecular weight (Mw) = 12 000 Da) and 75:25 PLGA (Resomer® RG752, Mw = 12 000 Da) were obtained from Boehringer Ingelheim (Ingelheim, Germany) and poly(D,L-lactide) (D,L-PLA 2 M, Mw = 22 000 Da) was received from Alkermes (Cincinnati, OH, USA). The Mw determined by gel permeation chromatography were reported in Table 3. Meso-tetra(p-hydroxyphenyl)porphyrin (p-THPP) provided by Aldrich (Steinheim, Germany) was chosen as photosensitizer (Fig. 1). Poly(vinyl alcohol) (PVAL) 87.7% hydrolyzed with a Mw of 26 000 Da (Mowiol® 4–88, Hoechst, Frankfurt/Main, Germany) was selected as stabilizing agent. Benzyl alcohol (Fluka Biochemika, Buchs, Switzerland) was chosen as the organic partially water-miscible solvent. The choice of the solvent was dictated by the photosensitizer solubility and the acceptability of solvent residues in parenteral formulations. D(+)-trehalose dihydrate (Sigma, St. Louis, MO, USA) was used as lyoprotectant.

All other chemicals were of analytical grade and used without further purification.

2.2. Methods

2.2.1. Nanoparticle preparation by the emulsification-diffusion technique

The nanoparticles were produced by the emulsification-diffusion technique as previously described [22]. Typically, 6 g of organic phase consisting of the polymer dissolved in benzyl alcohol were emulsified with 8 g of aqueous PVAL solution (17% (w/w)). After 15 min of mechanical stirring at 2000 rpm, 500 ml of distilled water were added to the resulting emulsion in order to allow the complete diffusion of the benzyl alcohol into the aqueous external phase, leading to the formation of nanoparticles. To produce the p-THPP-loaded nanoparticles, a known amount of the photosensitizer was dissolved into the organic phase before the emulsification. Finally, the nanoparticle dispersions were purified by cross-flow filtration as described in a previously [21] using a Sartocon® Slice device fitted with an ultrafiltration membrane (cut-off of 300 000 Da, Sartorius, Goettingen, Germany). The p-THPP-loaded nanoparticle formulations were protected from light during the production process.

2.2.2. Particle size analysis

The nanoparticle mean size and the polydispersity index (PI) were assessed by photon correlation spectroscopy using a Zetasizer® 5000 (Malvern, Worcestershire, England). The PI is an indication of the size distribution with values ranging from 0 to 1. Size measurements were carried out at different steps of the nanoparticle production. Redispersion was carried out in different media including distilled water, fetal bovine serum (FBS) (Gibco®, Life Technologies, Switzerland), phosphate buffer saline (PBS) (Gibco®, Life Technologies, Switzerland), Waymouth growth medium (Gibco®, Life Technologies, Switzerland) and human plasma. The measurements were performed in triplicate for all batches.

2.2.3. Sterile filtration

Nanoparticle suspensions were first pre-filtered through a membrane with a pore size of 0.45 μm (Millipore®, Volketswil, Switzerland). Then, the suspensions were sterilized by filtering through a Steriflip® filter unit with a 0.22 μm Millipore Express™ membrane (Millipore®, Volketswil, Switzerland). In order to determine the loss of drug by adsorption on to the membrane filter, the drug loading and the entrapment efficiency were determined before and after the sterilization procedure.

2.2.4. Sterility testing

Sterility testing was performed on the nanoparticle suspensions immediately after sterilization and on the final freeze-dried nanoparticles, following European Pharmacopoeia guidelines (addendum 1999). As described in earlier work [21], membrane filtration followed by incubation of the membrane in culture media was chosen as the testing method. Thioglycollate resazurine broth (BioMérieux®, Marcy, France) was used as an aerobic or anaerobic medium for the detection of bacteria and tripcase soy broth (BioMérieux®, Marcy, France) was used as medium for the detection of yeasts and fungi. The validation of the sterility testing was also performed according to the same protocol.

2.2.5. Freeze-drying

The sterile nanoparticle suspensions were poured into pre-weighed glass vials under laminar-hood and frozen in a cold ethanol bath (−60°C) for 30 min. Freeze-drying was carried out in an non-aseptic area as previously described [21] using an LSL Secfroid lyophilizer, model Lyolab CII (Secfroid, Aclens, Switzerland) at 0.001 Bar. The freeze-dried samples were then aliquoted in sealed vials under aseptic conditions and filled with an inert gas such as argon through a 0.22 μm filter (Minisart®, Millipore, Switzerland). The samples were stored at 8°C before analysis.

2.2.6. Determination of the residual moisture by Karl-Fischer titration

The residual moisture contents in freeze-dried powders were determined by Karl-Fischer titration. The assays were performed by means of a Mettler DL 18 Karl-Fischer colorimetric Titrator (Mettler-Toledo, Greifensee, Switzerland), calibrated with anhydrous methanol (Hydranal®, Riedel-de Häen AG, Seelze, Germany). The moisture content of the nanoparticle powders was monitored in triplicate.

2.2.7. Determination of zeta potential

The measurements of zeta potential were performed using the technique of electrophoretic laser Doppler anemometry using a Malvern Zetasizer® 5000 (Malvern, Worcestershire, England). Since these nanoparticle formulations are subsequently intended for in vitro phototoxicity studies on EMT-6 mammary tumor cells, the Waymouth growth medium (Gibco®, Life Technologies, Basle, Switzerland) supplemented with 10% (v/v) of FBS (Gibco®, Life Technologies, Basle, Switzerland), was chosen as medium for the zeta potential determination. The values reported are the mean value ± standard deviation (SD) for six values. In parallel, a standard latex (−50 mV) was used to test the reliability of the measurements.

2.2.8. Determination of residual PVAL on the nanoparticles

It has been observed that, after the cross flow filtration procedure, a certain amount of PVAL remains at the surface of the particles, irrespective of the volume of water used [28]. Therefore, the residual amount of PVAL was determined. Typically, 4 mg of nanoparticles freeze-dried without trehalose were dispersed in 5.0 ml of tetrahydrofuran (THF, Merch, Darmstadt, Germany). All compounds with the exception of PVAL were dissolved. The solution was then filtered on a membrane filter (Durapore®, 0.45 μm, Millipore®, Switzerland) and any residual PVAL was retained on the filter. The filter was rinsed three times with 5 ml of THF. In order to verify that no drug remained after the washing procedure, the absorption of the final rinsing solution was determined at 653 nm. Five milliliters of hot pure distilled water (94°C) were added to the filter and the PVAL was dissolved under sonication. The resulting solution was adjusted to 10.0 ml with distilled water. An aliquot of this solution was treated with 7.5 ml of a 4% (w/w) boric acid solution and 1.5 ml of an iodine solution (1.27% (w/w) iodine and 2.5% (w/w) potassium iodide in water) to form a soluble complex. Iodine forms a polyiodide ion, which is incorporated in coiled PVAL chains and causes blue colouring [29]. The absorbance was measured at 644 nm. All determinations were performed in triplicate.

2.2.9. Determination of drug loading and entrapment efficiency

An accurately weighed amount of nanoparticles, freeze-dried without lyoprotectant, was dissolved in 5.0 ml of THF under magnetic stirring for 30 min. The amount of p-THPP encapsulated was assayed using a spectrophotometer at 653 nm. The drug loading and the entrapment efficiency were calculated in the following manner.

$$\text{Drug loading} = \frac{\text{Amount of photosensitizer in nanoparticles}}{\text{Amount of nanoparticles}} \times 100$$

$$\text{Entrapment efficiency} = \frac{\text{Drug loading}}{\text{Theoretical drug loading}} \times 100$$

The determinations were performed in triplicate.

2.2.10. X-ray diffraction analysis

The crystallinity of both polymer and p-THPP was determined by X-ray powder diffraction using a Guinier Enraf-Nornius FR552 camera (Cu $K_{\alpha 1}$ radiation) (Phillips, Netherlands). The powder patterns recorded on a film, were digitized with an LS-18 line scanner. The assay was carried out on polymers, free p-THPP, p-THPP-loaded nanoparticles (9–12% (w/w)) and physical mixtures of p-THPP and unloaded nanoparticles of each formulation (9–12% (w/w)).

2.2.11. Determination of the polymer molecular weight by gel permeation chromatography (GPC)

The molecular weight of the polymer before and after the nanoparticle preparation was assessed on a Waters 771 GPC equipped with three Styragel columns (HR 1, HR 2, HR 4) (Waters Rupperswil, Switzerland) in series. THF was used as the mobile phase and the following setting parameters were used: injected volume 200 μl; sample concentration 0.25% (w/v); temperature of columns 30°C; flow-rate 1.0 ml/min. The system was calibrated using monodisperse polystyrene standards (Tosoh, Corporation) of the following

molecular weights: 500, 2630, 5970, 9100, 18 100 and 37 900 Da. The molecular mass was expressed by the average Mw and the Mw distribution (i.e. average molecular weight/average molecular number ratio (MW/MH ratio)).

3. Results and discussions

3.1. Nanoparticle preparation

The choice of encapsulation method was dictated by the solubility characteristics of both p-THPP and the polymers. In this study, the emulsification-diffusion technique was selected. The optimal parameters for the preparation of sub-150 nm nanoparticles were determined based on previous works [21,22]. Three polyesters were chosen for this work: 50:50 PLGA, 75:25 PLGA and PLA. The polymers were chosen on the basis of their varying lactic acid: glycolic acid ratio yet similar molecular weight range and crystallinity. The copolymer molar ratio, which in turn dictates polymer hydrophilicity has been shown to influence nanoparticle behaviour such as drug release and biodegradation rate [30]. The mean sizes of the nanoparticles are reported in Table 1. As determined by photon correlation spectroscopy, the raw nanoparticle mean size was in the range of 93–157 nm and showed good reproducibility. For all nanoparticle formulations obtained, the PI was lower than 0.1 (data not shown), which indicated a narrow particle size distribution. The encapsulation of p-THPP into the

Table 1
Surface characterization of purified nanoparticles (mean ± SD, $n = 3$ for residual PVAL and particle mean size, $n = 6$ for zeta potential)

| Initial drug loading (%)	50:50 PLGA		
	Particle mean size (nm)	Residual PVAL (%)	Zeta potential (mV)
0	124 ± 2	15.9 ± 1.0	−5.3 ± 1.0
5	145 ± 1	17.6 ± 0.2	−5.3 ± 1.9
10	109 ± 3	24.1 ± 1.2	−4.7 ± 1.4
15	93 ± 0	33.5 ± 0.5	−5.2 ± 0.4
20	136 ± 2	38.3 ± 4.2	−5.8 ± 0.3
	75:25 PLGA		
	Particle mean size (nm)	Residual PVAL (%)	Zeta potential (mV)
0	132 ± 12	14.5 ± 7.0	−5.1 ± 0.7
5	157 ± 7	19.2 ± 1.1	−4.3 ± 0.6
10	118 ± 4	24.1 ± 2.5	−4.2 ± 0.7
15	95 ± 6	34.8 ± 0.5	−6.6 ± 1.9
20	99 ± 0	35.5 ± 1.2	−4.9 ± 0.8
	PLA		
	Particle mean size (nm)	Residual PVAL (%)	Zeta potential (mV)
0	112 ± 1	19.3 ± 0.3	−7.8 ± 1.1
5	116 ± 2	21.7 ± 0.1	−5.6 ± 0.8
10	134 ± 6	24.9 ± 16.9	−4.3 ± 0.8
15	104 ± 1	28.3 ± 4.0	−5.0 ± 0.6
20	109 ± 1	45.3 ± 6.0	−4.8 ± 0.6
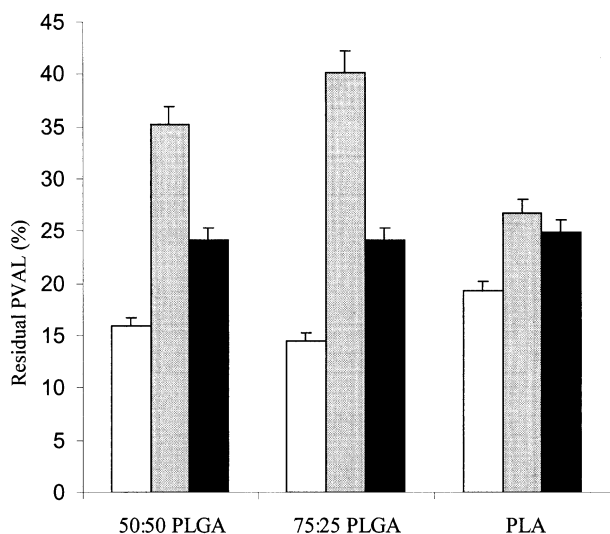
Fig. 2. Influence of the washing water volume on the percentage of residual PVAL: (□) blank nanoparticles purified with 4 L of distilled water, (▦) p-THPP-loaded nanoparticles purified with 4 L of distilled water, (■) p-THPP loaded nanoparticles purified with 10 L of distilled water (mean ± SD, $n = 3$).

nanoparticles did not significantly affect particle size even at relatively high drug loadings (Table 1). This is in accordance with a study performed by Tsai et al. [31], where despite an increase in the drug loading from 3.65 to 13.80%, no influence on the mean particle size was observed. On the other hand, it has been reported that an increase in procaine hydrochloride loading from 1 to 10% (w/w) led to an increase in particle size from 157.1 to 209.5 nm while a decrease in particle size from 148.3 to 20.2 nm was observed with procaine dihydrate [23].

3.2. Purification and surface characterization of the nanoparticles

Cross-flow filtration was used for the purification of the raw nanoparticle suspensions. It has been established that the amount of residual PVAL remaining at the nanoparticle surface is directly related to the specific surface area of the particles [32,33]. In this study, this relationship could be only verified for drug-free nanoparticles. For the p-THPP loaded nanoparticles, the PVAL content was influenced by

other factors such as the drug loading. As shown in Fig. 2, after purification of the drug-free nanoparticle formulations with 4 L of distilled water, residual PVAL amounted to 15.9 ± 1.0, 14.5 ± 7.0 and 19.3 ± 0.3% (w/w) for 50:50 PLGA, 75:25 PLGA and PLA, respectively. These results are consistent with those established in a previous study [21]. However, for the p-THPP-loaded nanoparticles, the residual PVAL remaining in the suspensions was 35.2 ± 1.0, 40.2 ± 1.8 and 26.7 ± 3.0% (w/w) for 50:50 PLGA, 75:25 PLGA and PLA nanoparticles, respectively (Fig. 2). Reduction of the level of residual PVAL was achieved by increasing the volume of the washing water to 10 L. The residual PVAL amounts were decreased to 24% (w/w) for all p-THPP-loaded nanoparticle formulations (Fig. 2), whereas a slight increase in the mean particle size and the PI were observed (data not shown). Since the particles need to be sterilized by membrane filtration, an increase in the particle size and PI was undesirable since this could impede membrane filtration by clogging the membrane. The high percentage of residual PVAL might be related to the presence of the photosensitizer. Indeed, the drug seems to demonstrate a certain affinity to this hydrophilic stabilizing colloid inducing the adsorption of PVAL on the particle surface. The amount of PVAL remaining in these formulations could be acceptable due to the widespread use of this polymer in diverse applications for human use. Indeed, numerous studies have demonstrated that PVAL is an excellent material for use in medical applications such as drug delivery devices due to its biocompatibility [34]. However, since PVAL is non-biodegradable, accumulation in tissues or organs should be avoided to present toxicity. Nevertheless, it has been reported that the plasma half-life of PVAL after intravenous injection depends on its molecular weight. The clearance of low Mw PVAL was rapid compared to those of high Mw [35,36]. Indeed, the half-life in the circulation was prolonged from 90 min (Mw 14 800) to 23 h (Mw 170 000) and the accumulation in most organs (e.g. liver) was very small [35].

The results of surface charge measurements are reported in Table 2. For all the polymers used, the unloaded and p-THPP-loaded nanoparticles exhibited similar low zeta potentials ranging from −4.2 to −7.8 mV. Generally,

Table 2

Influence of the theoretical drug loading on the effective drug loading and entrapment efficiency of p-THPP into polyester nanoparticles (mean ± SD, $n = 3$)

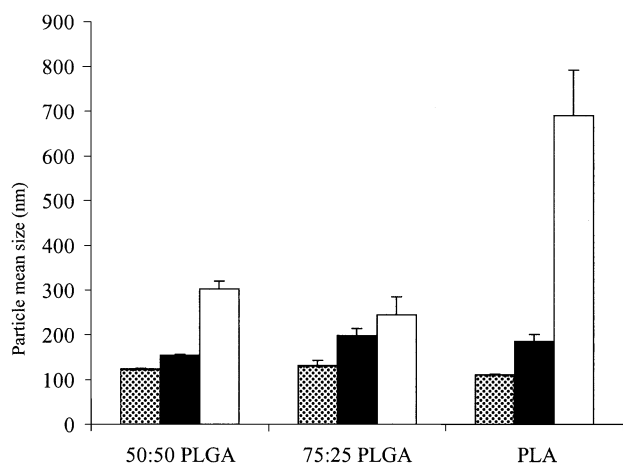| Initial drug loading (%)	50:50 PLGA		75:25 PLGA		PLA	
	Drug loading (%)	Entrapment efficiency (%)	Drug loading (%)	Entrapment efficiency (%)	Drug loading (%)	Entrapment efficiency (%)
5	3.8 ± 0.1	76.3 ± 1.4	3.9 ± 0.1	75.4 ± 2.6	4.6 ± 0.3	91.1 ± 6.4
10	7.8 ± 0.3	76.9 ± 3.4	8.1 ± 0.7	77.0 ± 7.0	7.3 ± 0.7	72.8 ± 8.7
15	9.4 ± 0.2	62.2 ± 1.1	9.2 ± 0.1	61.4 ± 0.5	9.2 ± 0.1	61.2 ± 0.5
20	11.3 ± 2.1	56.2 ± 10.5	9.5 ± 0.7	47.0 ± 3.2	12.7 ± 0.5	62.1 ± 2.6

Fig. 3. Mean size of nanoparticles: (▦) before freeze-drying, (■) after freeze-drying in the presence of the trehalose and reconstitution, (□) after freeze-drying without trehalose and reconstitution (mean ± SD, $n = 3$).

highly negative zeta potential values are expected for pure polyester nanoparticles due to the presence of carboxyl groups on the polymeric chain extremities [23]. However, in this study, the zeta potential values close to zero are due to the residual PVAL on the nanoparticle surface. Creating a shield between the nanoparticle surface and the surrounding medium, PVAL would mask the possible charged groups existing on the particle surface [37,38].

3.3. Redispersibility of freeze-dried nanoparticles

After freeze-drying, the nanoparticle cakes were first analyzed in terms of redispersibility and reconstitution rate. Manual shaking (30 s) was used for this study because injectable drugs that require reconstitution should be rapidly and easily prepared [39]. For the unloaded nanoparticles, substantial aggregation was observed after freeze-drying in the absence of a lyoprotectant (Fig. 3). The aggregation problem was overcome by using trehalose as a lyoprotectant at a weight ratio of 2:1 (2 g trehalose/1 g nanoparticles). This non-reducing disaccharide has previously exhibited a satisfactory lyoprotective effect for pharmaceutical and biological materials [21,40,41]. For all rehydrated unloaded nanoparticles, acceptable particle sizes for intravenous injection were obtained (Fig. 3). For p-THPP-loaded nanoparticles, different media were used for the redispersibility study because they were intended for use in subsequent experiments. As shown in Fig. 4, almost complete redispersion of the p-THPP-loaded nanoparticles freeze-dried with trehalose was achieved for all formulations except in human plasma, where a slight increase in the particle size was observed. Redispersion of the p-THPP loaded nanoparticles without trehalose could also be achieved after 1 h of vigorous stirring (Vortex-Genie 2, Scientific Industrie, Geneva, Switzerland) (data not shown). This may be attributed to the high amount of residual PVAL, which would act as wetting
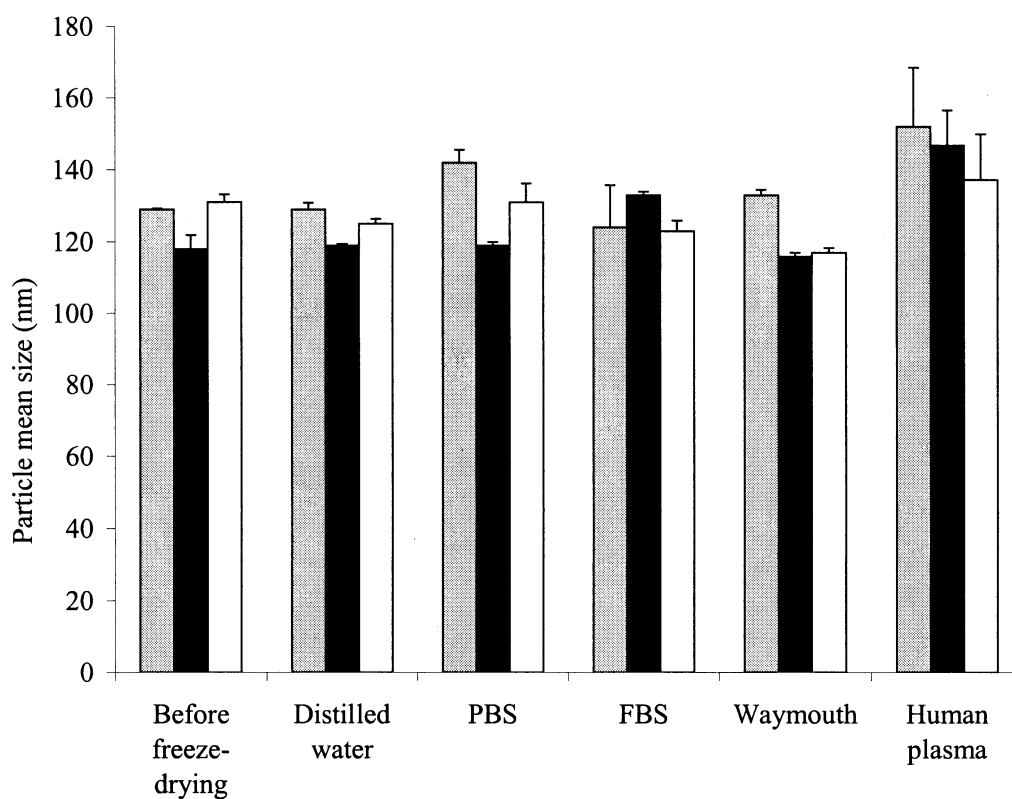

Fig. 4. Mean size of the freeze-dried p-THPP-loaded nanoparticles redispersed in different media (i.e. distilled water; PBS; FBS; Waymouth medium; human plasma): (▦) 50:50 PLGA, (■) PLA, (□) 75:25 PLGA (mean ± SD, $n = 3$). The particles were freeze-dried in presence of trehalose.
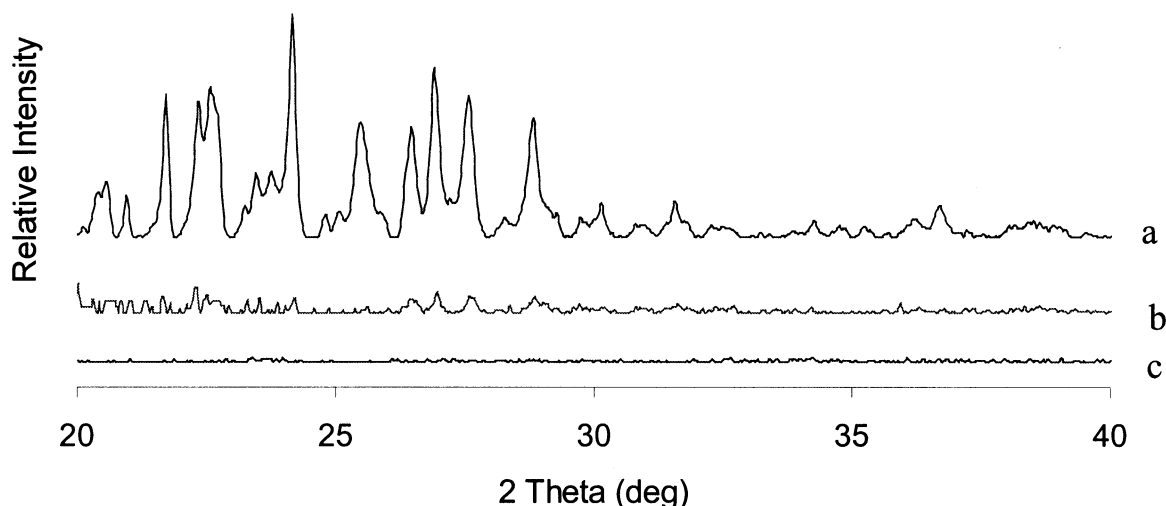
Fig. 5. X-ray powder diffraction pattern (Cu K$_{\alpha 1}$) of: (a) p-THPP; (b) physical mixture of p-THPP and PLA (12% (w/w)); and (c) p-THPP-loaded PLA nanoparticles (drug loading of 12% (w/w)).

agent during the particle rehydration under energic stirring conditions [40,42]. The freeze-dried powders were very hygroscopic due to the presence of the lyoprotectant, and therefore, suitable care had to be taken to avoid moisture contamination during the handling of the samples. The residual moisture levels immediately after the freeze-drying process amounted to 4.2 ± 0.8 and $5.1 \pm 0.5\%$ (w/w) for unloaded and p-THPP-loaded nanoparticles, respectively. This residual moisture is partly related to the unfrozen water trapped in the trehalose matrix during the sublimation drying step; the values reported here are consistent with those generally found in this type of dried products [39]. In order to keep the products under low relative humidity, the samples were stored according to recommendations described in other studies [39,40,43]. The dry cakes were immediately aliquoted in sealed light-protected sterile containers, which were filled with a dry and inert gas such as pure argon through a 0.22 μm sterile filter. Particulate and bacterial contamination could therefore be avoided. The photosensitizer was also stabilized by the removal of oxygen since oxygen plays an important role in many photochemical reactions [43]. Under these conditions, the final products were stable in terms of mean particle size and drug loading over a period of more than 6 months.

3.4. Nanoparticle sterilization, validation and sterility testing

In earlier work [21], we have established that Steriflip® filter units with a 0.22 μm Millipore Express™ membrane (modified polyethersulfone surface) provide satisfactory results in terms of flow rate, filtering capacity under vaccum and minimum material adsorption on the membrane. Determination of drug loading and entrapment efficiency before and after filtration showed no significant loss of drug by absorption on to the membrane (data not shown). Moreover,

after the sterile filtration, there was no significant change in particle size and size distribution (data not shown). The results of the sterility testing performed after sterile filtration and freeze-drying showed no turbidity of the media during the incubation period attesting to the sterility of the final nanoparticulate formulations. Prior to sterility testing of the filtered preparations, the potential antimicrobial activity of p-THPP and the formulation excipients, if any, was determined. In practical terms, the micro-organism proliferation must be produced to the point where the liquid medium becomes visibly cloudy. For all organisms, proliferation was observed in every media containing the tested p-THPP-loaded nanoparticulate formulations. These results demonstrated that under these conditions, p-THPP did not exhibit a bacteriostatic or fungistatic activity.

3.5. Effect of the initial drug loading

To increase the drug loading in the nanoparticles, the amount of p-THPP in the formulations was varied from 5 to 20% (w/w). The results (Table 2) showed that the drug loading increased from 3.8 up to 11% (w/w) while a decrease in the corresponding drug entrapment efficiency was observed. The same trend was observed with the three polymers tested. These results were somewhat surprising. The effect of polymer hydrophobicity on entrapment of the ovalbumin was reported by Jeffery et al. [44]. In this study, more hydrophobic polyesters (lactide-rich polyesters) showed relatively lower entrapment levels compared to more hydrophilic polyesters (glycolide-rich polyesters). However, in the present study, such relationship in the entrapment efficiency with respect to polymer composition (PLGA versus PLA) could not be clearly established. One of the goals of this study was to obtain nanoparticulate formulation of p-THPP with optimal properties in terms of size integrity, drug loading, entrapment efficiency and to minimize drug loss during the nanoparticle preparation.

Table 3
GPC characterization of the polymers and of the unloaded nanoparticles

Polymer	Theoretical Mw[a]	PLA:PGA ratio[a]	Cristanillity[a]	Polymer			Nanoparticles		
				Mw[b]	Mn[b]	PI[b]	Mw[b]	Mn[b]	PI[b]
RG502	12 000	50: 50	Amorphous	13 600	7010	1.95	12 500	7410	1.69
RG752	12 000	75: 25	Amorphous	15 900	7660	2.07	15 500	8690	1.78
PLA	22 000	100: 0	Amorphous	19 000	10 400	1.82	18 400	11 070	1.66

[a] Data from the manufacters.
[b] Data measured by GPC.

Nanoparticle formulations characterized by a 10% (w/w) theoretical drug loading will be used in the future for in vitro PDT studies.

3.6. X-rays analysis

The physical state of both polymers and p-THPP incorporated into nanoparticles was established by X-ray analysis. The results given in Fig. 5 show that the p-THPP in the physical mixture exhibited the same crystal lattice as pure macroscopic p-THPP crystals. In spite of a lower relative intensity, the diffraction pattern of the physical mixture (12% (w/w)) could be superimposed on the pattern of the pure p-THPP. In contrast, the X-ray pattern of the p-THPP-loaded nanoparticles did not show any diffraction peaks. This might be an indication of an amorphous state or of a molecularly dispersed state of the photosensitizer within the polymer matrix. Similar patterns without diffraction peaks were also observed in both polymers and unloaded nanoparticles, which confirmed the amorphous state of these polymers (data not shown).

3.7. Polymer molecular weight analysis

In order to assess the effect of physical stress during the preparation process on the Mw and Mw distribution of the polymer, these parameters were measured by GPC for both the polymer and the unloaded nanoparticles. As shown in Table 3, the Mw distribution obtained with all polymers tested was higher than 1.6, indicating certain dispersion due to the presence of different chain lengths and range of molecular weights [45]. The Mw determined were relatively different from the theoretical values (Table 3). For all types of the unloaded nanoparticles tested, the Mw and the Mw distribution were modified in terms of a slight decrease whereas the Mn were increased. This decrease in the molecular mass distribution resulted from an increase in the number of short polymer chains caused by scission of the large chains during the particle preparation procedure.

4. Conclusions

In this study, it has been demonstrated that p-THPP can be encapsulated into sub-150 nm polyester nanoparticles with high drug loadings and entrapment efficiencies. The copolymer molar ratio has been frequently shown to influence strongly the behaviour of the nanoparticles. However, in the present study, the polymer composition did not appear to affect significantly the physical characteristic of the nanoparticles. Indeed, irrespective of the polymer composition, the p-THPP-loaded nanoparticles exhibited the same characteristics in terms of particle size, surface characteristics and redispersibility. Nevertheless, respect to the particle surface characteristics, the percentage of residual PVAL (reaching up to 45%) was strongly found to be dependent on the drug loading. Such residual amounts of PVAL may be acceptable in injectable formulations since PVAL is considered to be biocompatible and a high clearance of low Mw PVAL from the body has been observed after intravenous injection. It was also shown that sterilization of the nanoparticles by membrane filtration was possible. This is a great advantage for many incorporated drugs such as photosensitizing agents, which may be denatured by heat or gamma sterilization.

The present work forms the foundations of subsequent studies, which are aiming to evaluate the photodynamic activity of p-THPP-loaded nanoparticles on EMT-6 mammary tumor cells. This subsequent work will help in determining the impact of copolymer molar ratio on the particle properties.

References

[1] R.K. Pandey, A.B. Sumlin, S. Constantine, M. Aoudia, W.R. Potter, D.A. Bellnier, B.W. Henderson, M.A. Rodgers, K.M. Smith, T.J. Dougherty, Alkyl ether analogs of chlorophyll-a derivatives: Part I. Synthesis, photophysical properties and photodynamic efficacy, Photochem. Photobiol. 64 (1996) 194–204.
[2] B.W. Henderson, D.A. Bellnier, W.R. Greco, A. Sharma, R.K. Pandey, L.A. Vaughan, K.R. Weishaupt, T.J. Dougherty, An in vivo quantitative structure-activity relationship for a congeneric

series of pyropheophorbide derivatives as photosensitizers for photo-dynamic therapy, Cancer Res. 57 (1997) 4000–4007.

[3] J.P. Rovers, A.E. Saarnak, M. de Jode, H.J.C.M. Sterenborg, O.T. Terpstra, M.F. Grahn, Biodistribution and bioactivity of tetra-pegy-lated meta-tetra(hydroxyphenyl)chlorin compared to native meta-tetra(hydroxyphenyl)chlorin in a rat liver tumor model, Photochem. Photobiol. 71 (2000) 210–217.

[4] J. Kopecek, P. Kopeckova, T. Minko, Z.-R. Lu, C.M. Peterson, Water soluble polymers in tumor targeted delivery, J. Control. Rel. 74 (2001) 147–158.

[5] A.M. Richter, E. Waterfield, A.K. Jain, J.A. Canaan, B.A. Allison, J.G. Levy, Liposomal delivery of a photosensitizer benzoporphyrin derivative monoacid ring A (BPD), to tumor tissue in a mouse tumor model, Photochem. Photobiol. 57 (1993) 1000–1006.

[6] U. Isele, P. van Hoogevest, R. Hilfiker, H.G. Capraro, K. Schieweck, J.G. Levy, H. Leuenberger, Large-scale production of liposomes containing monomeric zinc phthalocyanine by controlled dilution of organic solvents, J. Pharm. Sci. 83 (1994) 1608–1616.

[7] A.R. Morgan, G.M. Garbo, R.W. Keck, S.H. Selman, New photosen-sitizers for photodynamic therapy: combined effect of metallopur-purin derivatives and light on transplantable bladder tumors, Cancer Res. 48 (1988) 194–198.

[8] G.M. Garbo, V.H. Fingar, T.J. Wienman, E.B. Noakes III, P.S. Haydon, P.B. Cerrito, D.H. Kessel, A.R. Morgan, In vivo and in vitro photodynamic studies with benzochlorin imimium salts deli-vered by a lipid emulsion, Photochem. Photobiol. 64 (1998) 561–568.

[9] J. Taillefer, M.-C. Jones, N. Brasseur, J.E. Van Lier, J.C. Leroux, Preparation and characterization of pH-responsive polymeric micelles for the delivery of photosensitizing anticancer drugs, J. Pharm. Sci. 89 (2000) 52–62.

[10] N. Brasseur, D. Brault, P. Couvreur, Adsorption of hematoporphyrin onto polyalkylcyanoacrylate nanoparticles: carrier capacity and drug release, Int. J. Pharm. 70 (1991) 129–135.

[11] V. Lenaerts, A. Labib, F. Chouinard, J. Rousseau, H. Ali, J.E. Van Lier, Nanocapsules with a reduced liver uptake: targeting of phthalo-cyanines to EMT-6 mouse mammary tumour in vivo, Eur. J. Pharm. Biopharm. 41 (1995) 38–43.

[12] E. Allémann, N. Brasseur, O. Benrezzak, J. Rousseau, S.V. Kudre-vich, R.W. Boyle, J.C. Leroux, R. Gurny, J.E. Van Lier, PEG-coated poly(lactic acid) nanoparticles for the delivery of hexadecafluoro zinc phthalocyanine to EMT-6 mouse mammary tumours, J. Pharm. Phar-macol. 47 (1995) 382–387.

[13] J. Kristl, E. Allémann, R. Gurny, Formulation and evaluation of zinc-phthalocyanine-loaded poly(D,L-lactic acid) nanoparticles, Acta Pharm. 46 (1996) 1–12.

[14] O. Bourdon, V. Mosqueira, Ph. Legrand, J. Blais, A comparative study of the cellular uptake, localization and phototoxicity of meta-tetra(hydroxyphenyl)chlorin encapsulated in surface-modified submi-cronic oil/water carriers in HT29 tumor cells, J. Photochem. Photo-biol. B Biol. 55 (2000) 164–171.

[15] H.S. Yoo, K.H. Lee, J.E. Oh, T.G. Park, In vitro and in vivo anti-tumor activities of nanoparticles based on doxorubicin-PLGA conju-gates, J. Control. Rel. 68 (2000) 419–431.

[16] G.M. Barratt, Therapeutic applications of colloidal drug carriers, Pharm. Sci. Technol. Today 3 (2000) 163–171.

[17] R.L. Juliano, Factors affecting the clearance kinetics and tissue distri-bution of liposomes, microspheres and emulsions, Adv. Drug Deliv. Rev. 2 (1988) 31–54.

[18] K. Maruyama, O. Ishida, T. Takizama, K. Moribe, Possibility of active targeting to tumor tissues with liposomes, Adv. Drug Deliv. Rev. 40 (1999) 89–102.

[19] G. Poste, R. Kirsh, B.A. Allison, Site-specific (targeted) drug delivery in cancer therapy, Biotechnology 1 (1983) 869–878.

[20] G. Kong, R.D. Braun, M.W. Dewhirst, Hyperthermia enables tumor-specific nanoparticle delivery: effect of particle size, Cancer Res. 60 (2000) 4440–4445.

[21] Y.N. Konan, R. Gurny, E. Allémann, Preparation and characterization

[22] J.C. Leroux, E. Allémann, E. Doelker, R. Gurny, New approach for the preparation of nanoparticles by an emulsification-diffusion method, Eur. J. Pharm. Biopharm. 41 (1995) 14–18.

[23] T. Govender, S. Stolnik, M.C. Garnett, I. Illum, S.S. Davis, PLGA nanoparticles prepared by nanoprecipitation: drug loading and release studies of a water soluble drug, J. Control. Rel. 57 (1999) 171–185.

[24] M.C. Berenbaum, S.L. Akande, R. Bonnett, H. Kaur, S. Ioannou, meso-Tetra(hydroxyphenyl)porphyrins, a new class of potent tumour photo-sensitizers with favourable selectivity, Br. J. Cancer 54 (1986) 717–725.

[25] R. Bonnett, R.D. White, U.-J. Winfield, M.C. Berenbaum, Hydropor-phyrins of the meso-tetra(hydroxyphenyl)porphyrin series as tumour photosensitizers, Biochem. J. 261 (1989) 277–280.

[26] J.M. Anderson, M.S. Shive, Biodegradation and biocompatibility of PLA and PLGA microspheres, Adv. Drug Deliv. Rev. 28 (1997) 5–24.

[27] R.L. Dunn, J.P. English, J.D. Strobel, D.R. Cowsar, T.R. Tice, Preparation and evaluation of lactide/glycolide copolymers for drug delivery, in: C. Migliaresi (Ed.), Polymers in Medicine III, Elsevier Science Publishers BV, Amsterdam, 1988, pp. 149–160.

[28] E. Allémann, E. Doelker, R. Gurny, Drug loaded poly(lactic acid) nanoparticles produced by a reversible salting-out process: purifica-tion of an injectable dosage form, Eur. J. Pharm. Biopharm. 39 (1993) 13–18.

[29] I. Sakurada, Chemical Reactions of Polyvinyl Alcohol, International Fiber Science and Technology Series: Polyvinyl Alcohol Fibers, Marcel Dekker, Inc, New York, 1985, pp. 137–159.

[30] J.M. Anderson, M.S. Shive, Biodegradation and biocompatibility of PLA and PLGA microspheres, Adv. Drug Deliv. Rev. 28 (1997) 5–24.

[31] D.C. Tsai, S.A. Howard, T.F. Hogan, C.J. Malanga, S.J. Kandzari, J.K.H. Ma, Preparation and in vitro evaluation of polylactic acid-mitomycin C microcapsules, J. Microencapsul. 3 (1986) 191–193.

[32] E. Allémann, R. Gurny, E. Doelker, Preparation of aqueous polymeric nanodispersions by a reversible salting-out process: influence of process parameters on particle size, Int. J. Pharm. 87 (1992) 247–253.

[33] S.C. Lee, J.T. Oh, M.H. Jang, S.I. Chung, Quantitative analysis of polyvinyl alcohol on the surface of poly(D,L-lactide-co-glycolide) microparticles prepared by solvent evaporation method: effect of particle size and PVA concentration, J. Control. Rel. 59 (1999) 123–132.

[34] S. Mallapragada, S. McCarthy-Schroeder, Poly(vinyl alcohol) as a drug delivery carrier, in: D.L. Wise (Ed.), Handbook of Pharmaceu-tical Controlled Release Technology, Marcel Dekker, Inc, New York, 2000, pp. 31–46.

[35] T. Yamaoko, Y. Tabata, Y. Ikada, Comparison of body distribution of poly(vinyl alcohol) with other water-soluble polymers after intrave-nous administration, J. Pharm. Pharmacol. 47 (1995) 479–486.

[36] Y. Tabata, Y. Murakami, Y. Ikada, Tumor accumulation of poly(vinyl alcohol) of different sizes after intravenous injection, J. Control. Rel. 50 (1998) 123–133.

[37] D. Quintanar-Guerrero, H. Fessi, E. Allémann, E. Doelker, Influence of stabilizing agents and preparative variables on the formation of poly(D,L-lactic acid) nanoparticles by an emulsification-diffusion technique, Int. J. Pharm. 143 (1996) 133–141.

[38] T. Görner, R. Gref, D. Michelot, F. Sommer, M.N. Tran, E. Dellache-rie, Lidocaine-loaded biodegradable nanospheres. I. Optimization of the drug incorporation into the polymer matrix, J. Control. Rel. 57 (1999) 259–268.

[39] J.W. Snowman, Freeze drying of sterile products, in: M.J. Groves, W.P. Olson, M.H. Anisfeld (Eds.), Sterile Pharmaceutical Manufac-turing: Applications for the 1990's, Interpharm Press, Buffalo Grove, 1991, pp. 79–108.

[40] J.F. Carpenter, M.J. Pikal, B.S. Chang, T.W. Randolph, Rational design of stable lyophilized protein formulations: some practical advice, Pharm. Res. 14 (1997) 969–974.

[41] F. De Jaeghere, E. Allémann, J.C. Leroux, W. Stevels, J. Feijen, E. Doelker, R. Gurny, Formulation and lyoprotection of poly(lactic acid-

of sterile and freeze-dried sub-200 nm nanoparticles, Int. J. Pharm. 233 (2002) 239–252.

co-ethylene oxide) nanoparticles: influence on physical stability and in vitro cell uptake, Pharm. Res. 16 (1999) 859–866.

[42] H. Murakami, Y. Kawashima, T. Niwa, T. Hino, H. Takeuchi, M. Kobayashi, Influence of the degree of hydrolyzation and polymerization of poly(vinyl alcohol) on the preparation and properties of poly(D,L-lactide-co-glycolide) nanoparticle, Int. J. Pharm. 149 (1997) 43–49.

[43] H.H. Tonnesen, Formulation and stability testing of photolabile drugs, Int. J. Pharm. 225 (2001) 1–14.

[44] H. Jeffery, S.S. Davis, D.T. O'Hagan, The preparation and characterization of poly(lactide-co-glycolide) microparticles. II: The entrapment of a model protein using a (water-in-oil)-in-water emulsion solvent evaporation technique, Pharm. Res. 10 (1993) 362–368.

[45] R. Jain, N.H. Shah, A.W. Malick, C.T. Rhodes, Controlled drug delivery by biodegradable poly(ester) devices: different preparative approaches, Drug Dev. Ind. Pharm. 24 (1998) 703–727.